



# Effect of Oxygen Contamination on Propionate and Caproate Formation in Anaerobic Fermentation

Flávio C. F. Baleeiro<sup>1,2</sup>, Magda S. Ardila<sup>1,2</sup>, Sabine Kleinsteuber<sup>1</sup> and Heike Sträuber<sup>1\*</sup>

<sup>1</sup>Department of Environmental Microbiology, Helmholtz Centre for Environmental Research – UFZ, Leipzig, Germany, <sup>2</sup>Institute of Process Engineering in Life Science 2, Technical Biology, Karlsruhe Institute of Technology – KIT, Karlsruhe, Germany

## OPEN ACCESS

### Edited by:

David Strik,  
Wageningen University and Research,  
Netherlands

### Reviewed by:

Nathaniel W. Fortney,  
Great Lakes Bioenergy Research  
Center (DOE), United States  
Diana Calvo,  
Arizona State University, United States

### \*Correspondence:

Heike Sträuber  
heike.straeuber@ufz.de

### Specialty section:

This article was submitted to  
Bioprocess Engineering,  
a section of the journal  
Frontiers in Bioengineering and  
Biotechnology

**Received:** 15 June 2021

**Accepted:** 19 August 2021

**Published:** 10 September 2021

### Citation:

Baleeiro FCF, Ardila MS,  
Kleinsteuber S and Sträuber H (2021)  
Effect of Oxygen Contamination on  
Propionate and Caproate Formation in  
Anaerobic Fermentation.  
Front. Bioeng. Biotechnol. 9:725443.  
doi: 10.3389/fbioe.2021.725443

Mixed microbial cultures have become a preferred choice of biocatalyst for chain elongation systems due to their ability to convert complex substrates into medium-chain carboxylates. However, the complexity of the effects of process parameters on the microbial metabolic networks is a drawback that makes the task of optimizing product selectivity challenging. Here, we studied the effects of small air contaminations on the microbial community dynamics and the product formation in anaerobic bioreactors fed with lactate, acetate and H<sub>2</sub>/CO<sub>2</sub>. Two stirred tank reactors and two bubble column reactors were operated with H<sub>2</sub>/CO<sub>2</sub> gas recirculation for 139 and 116 days, respectively, at pH 6.0 and 32°C with a hydraulic retention time of 14 days. One reactor of each type had periods with air contamination (between 97 ± 28 and 474 ± 33 mL O<sub>2</sub> L<sup>-1</sup> d<sup>-1</sup>, lasting from 4 to 32 days), while the control reactors were kept anoxic. During air contamination, production of *n*-caproate and CH<sub>4</sub> was strongly inhibited, whereas no clear effect on *n*-butyrate production was observed. In a period with detectable O<sub>2</sub> concentrations that went up to 18%, facultative anaerobes of the genus *Rummeliibacillus* became predominant and only *n*-butyrate was produced. However, at low air contamination rates and with O<sub>2</sub> below the detection level, Coriobacteria and Actinobacteria gained a competitive advantage over Clostridia and Methanobacteria, and propionate production rates increased to 0.8–1.8 mmol L<sup>-1</sup> d<sup>-1</sup> depending on the reactor (control reactors 0.1–0.8 mmol L<sup>-1</sup> d<sup>-1</sup>). Moreover, *i*-butyrate production was observed, but only when Methanobacteria abundances were low and, consequently, H<sub>2</sub> availability was high. After air contamination stopped completely, production of *n*-caproate and CH<sub>4</sub> recovered, with *n*-caproate production rates of 1.4–1.8 mmol L<sup>-1</sup> d<sup>-1</sup> (control 0.7–2.1 mmol L<sup>-1</sup> d<sup>-1</sup>). The results underline the importance of keeping strictly anaerobic conditions in fermenters when consistent *n*-caproate production is the goal. Beyond that, micro-aeration should be further tested as a controllable process parameter to shape the reactor microbiome. When odd-chain carboxylates are desired, further studies can develop strategies for their targeted production by applying micro-aerobic conditions.

**Keywords:** carboxylate platform, lactate-based chain elongation, mixotrophy, micro-aerobic fermentation, open mixed culture, caproic acid, propionic acid, gas recirculation

## INTRODUCTION

Anaerobic fermentation with mixed microbial communities is an appealing option for the production of medium-chain carboxylates (MCCs) (De Groof et al., 2019). However, the high degree of complexity of mixed communities is an additional obstacle to achieve a stable and feasible bioprocess. Changes in operation parameters favor some microorganisms while negatively affecting others in ways that are hard to predict. Controlled experiments with defined substrates can help to understand the response of microbial networks to disturbances and to develop more robust fermentation processes (Angenent et al., 2016; Andersen et al., 2017; Oleskiewicz-Popiel, 2018).

Oxygen from the air can easily enter anaerobic reactors by diffusion due to incomplete tightness or oxic feedstocks, and is considered a disturbance of the anaerobic processes. At first thought, MCC-producing mixed cultures should be protected from O<sub>2</sub> at all costs. So far, almost all isolated MCC producers are strict anaerobes (one exception was described by Stamatopoulou et al. (2020)) to which O<sub>2</sub> causes damage *via* direct and indirect ways. O<sub>2</sub> gives rise to reactive oxygen species (ROS), such as O<sub>2</sub><sup>-</sup> and H<sub>2</sub>O<sub>2</sub>, which are intermediates produced during O<sub>2</sub> reduction that severely damage cells if not promptly neutralized (Johnson and Hug, 2019). Even though every cultured microorganism has mechanisms to deal with ROS (Johnson and Hug, 2019), obligate anaerobic bacteria such as *Clostridium* spp. suffer particularly from O<sub>2</sub> due to their high dependence on O<sub>2</sub>-sensitive enzymes (e.g., ferredoxin-dependent oxidoreductases or [FeFe]-hydrogenases) (Imlay, 2006; Khademian and Imlay, 2020). Most hydrogenases, which also contain Fe-S clusters, are reversibly or irreversibly inhibited by O<sub>2</sub> and its activated forms. Exposure to O<sub>2</sub> causes some hydrogenases to decompose or to form additional ROS that damage other parts of the cell (Stiebritz and Reiher, 2012).

Oxygen contamination does not necessarily mean a complete failure of the anaerobic process and its effect depends on the contamination rate and on the ability of the anaerobic community to remove the contaminant (Botheju and Bakke, 2011). Facultative anaerobic microorganisms present in mixed cultures can consume traces of oxygen and thus protect strict anaerobes (Nguyen and Khanal, 2018). As an exemplary proof of concept, the facultative anaerobe *Parageobacillus thermoglucosidasius* has been used for O<sub>2</sub> scrubbing before feeding waste gases to acetogenic cultures (Mohr et al., 2019). Additionally, the presence of biofilms, microbial aggregates, and other types of diffusion gradients in reactors can form protective oxygen barriers (Botheju and Bakke, 2011).

Uncontrolled aeration during anaerobic fermentation, e.g., *via* the supply of oxic substrates, can lead to the presence of strict aerobic microorganisms (Lambrecht et al., 2019). On the other hand, small amounts of oxygen may be desired in anaerobic processes. Micro-aeration, the controlled dosing of small amounts of air or oxygen (loosely defined from 5 to 5,000 mL O<sub>2</sub> L<sup>-1</sup> d<sup>-1</sup>), has been mainly used to create different oxidative-reductive regions in digesters to favor biological desulfurization (Krayzelova et al., 2015; Nguyen and Khanal, 2018). Besides, it has been reported that micro-aeration can enhance the hydrolysis

step in anaerobic digestion by increasing the production of extracellular enzymes such as proteases, amylases, and cellulases (Giroto et al., 2016). Presence of O<sub>2</sub> can also be advantageous in fermentations with acetogens. During batch cultivation of *Clostridium ljungdahlii* on H<sub>2</sub>, CO, CO<sub>2</sub>, and fructose, 8% O<sub>2</sub> in the headspace has been found to increase the production of ethanol (Whitham et al., 2015), which is an electron donor for chain elongation.

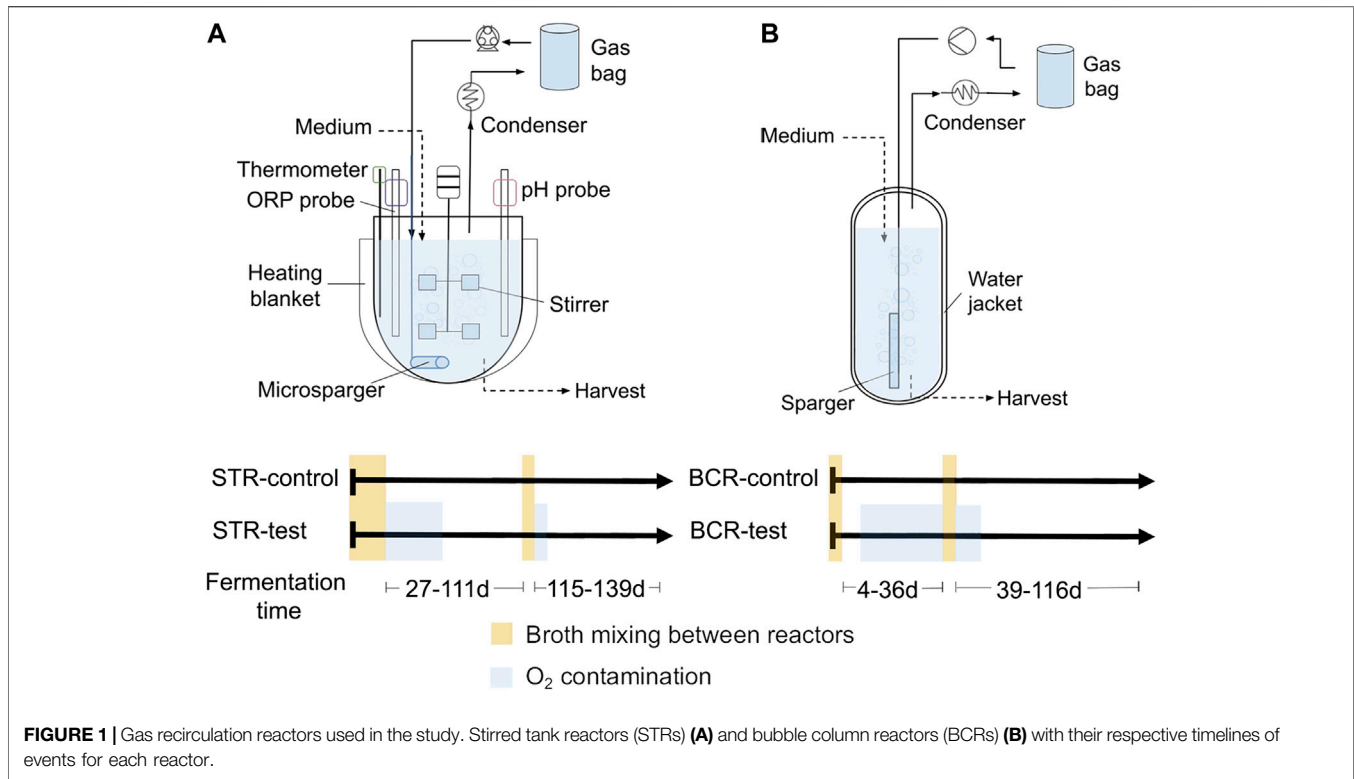
Although the possibilities with O<sub>2</sub> are being explored in many types of anaerobic technologies, no literature can be found about the effects of controlled O<sub>2</sub> contamination rates on chain elongation systems. One possible reason is that designing controlled experiments to understand the effects of small oxygen contamination in mixed microbial communities is not trivial. Distribution and monitoring of O<sub>2</sub> can be challenging at the low concentrations found in micro-aerated systems (Nguyen and Khanal, 2018). Recently, an anaerobic reactor system with continuous gas recirculation was presented as a way to ensure high gas availability to the microbial community at all times, while keeping the system closed and allowing to track component balances in the gas phase (Baleeiro et al., 2021b).

With the help of gas recirculation systems, this study aimed to investigate the effects of small air contamination on the dynamics of the microbial community and the product formation in MCC-producing fermenters. For this purpose, two stirred tank reactors (STRs) and two bubble column reactors (BCRs) with continuous H<sub>2</sub>/CO<sub>2</sub> recirculation were operated with mixed cultures fed with lactate and acetate. One of the reactors of each type had periods with air contamination, while the other two were kept anoxic.

## MATERIALS AND METHODS

### Experimental Design and Reactor Systems

Two pairs of reactors with continuous gas recirculation were assembled for this study. One pair consisted of stirred tank reactors (STR-control and STR-test) and the other of bubble column reactors (BCR-control and BCR-test). Assembly and configuration of the STRs were described in detail by Baleeiro et al. (2021b). BCRs were assembled and operated with the following differences in relation to the STRs: 1) the BCR vessels consisted of bubble columns made of glass with a working volume of 1.2 L each; 2) the systems had no oxidation-reduction potential (ORP) monitoring; 3) pH monitoring and correction was done manually three times a week; 4) temperature regulation was carried out *via* the water jacket of the vessels and a thermal bath; 5) gas recirculation was carried out with micro-diaphragm gas pumps NMP 830 (KNF Neuberger GmbH, Freiburg, Germany) at a flow of ca. 1.5 L min<sup>-1</sup>; and 6) an internal vertical hollow glass with holes of 1–2 mm was used to bubble the gas into the broth. In all other aspects, BCRs were operated similarly to STRs. The reactors were operated at 32°C, at pH values of 6.0 ± 0.1 (STRs) and 6.1 ± 0.3 (BCRs), and with a hydraulic retention time (HRT) of 14 days. The basal medium contained 133 mM lactate (12 g L<sup>-1</sup>) and 200 mM acetate (12 g L<sup>-1</sup>) as organic carbon sources and the gas reservoirs were periodically refilled with 10 L H<sub>2</sub>:CO<sub>2</sub> (80:20),



240 mL ethylene (methanogenesis inhibitor), and 120 mL He (tracer gas). Basal medium composition, reactor start-up and reactor operation were identical for STRs and BCRs and were as described by Baleeiro et al. (2021b), except that lactate was fed ten times per day along with the basal medium.

**Figure 1** shows the two reactor types used in the study and the timelines with the oxygen contamination events. The four reactors were inoculated with the broth harvested from the  $H_2/CO_2$ /ethylene recirculation reactors described by Baleeiro et al. (2021b). For STRs, the broths of the two reactors were mixed before the start of the experiment and before the second comparison period to ensure that both reactors started with identical microbial and chemical compositions for each comparison period. The same was done with the broths of the BCRs. Startup and broth mixing of STR-test and STR-control occurred on operation days 0–27 and the second broth mixture occurred on days 111–115 (**Figure 1A**). Startup and acclimatization of the community to a BCR occurred during the 86 days preceding the start of this study. Mixing of the BCR-control and BCR-test broths occurred on days 0–4 and 36–39 (**Figure 1B**). The broths were mixed without opening the reactors using Hei-Flow Precision peristaltic pumps (Heidolph Instruments GmbH, Schwabach, Germany), PVC tubes Tygon® LMT-55, and three-way valves. The major air contamination events were detected in STR-test on days 27–59 and 115–119 and in BCR-test on days 11–36 and 39–50 (**Figure 1**).

The reactors that remained air-tight all the time were used as control reactors. Reactors STR-test and BCR-test presented detectable air intrusion at certain periods due to imperfect air-tight conditions. With the help of a  $H_2$  leak detector (GLD-100, Coy Laboratory Products, Grass Lake, USA), tightness problems that caused gas to leak out of the reactor systems were located and promptly solved. The same was not true for tightness problems that only allowed air to leak into the system and that were solved by trial and error interventions.

## Analytical Methods

High performance liquid chromatography with a refractive index detector (HPLC Prominence-i RID, Shimadzu Europa GmbH, Duisburg, Germany) was operated under the conditions described by Apelt (2020) with adaptations described by Baleeiro et al. (2021a) for monitoring of the following chemicals in the aqueous phase: formate, acetate, ethanol, lactate, propionate, *n*-propanol, *n*-butyrate, *i*-butyrate, *n*-butanol, *n*-valerate, *i*-valerate, *n*-pentanol, *n*-caproate, *i*-caproate, *n*-hexanol, *n*-heptanoate, and *n*-caprylate. Biomass concentration was determined by measuring optical density at 600 nm (spectrophotometer Genesys 10 S, Thermo Scientific Inc., Waltham, United States). Conversion factors for optical density at 600 nm and biomass are described previously (Baleeiro et al., 2021a). In the gas phase,  $H_2$ ,  $CO_2$ ,  $CH_4$ , He,  $O_2$ ,  $N_2$ , and ethylene were monitored by gas chromatography as described by Logroño et al. (2020).

## Microbial Community Analysis

Microbial communities were analyzed by 16S rRNA gene amplicon sequencing with taxonomic assignments done with the SILVA 138 reference database (Yilmaz et al., 2014). DNA extraction, PCR, and library preparation for Illumina MiSeq sequencing were described previously (Baleeiro et al., 2021a). Trimming, filtering, and denoising of amplicon data as well as visualization of microbiome census data and Spearman correlations were done as described by Baleeiro et al. (2021a). All samples were rarified to an equal depth according to the sample with the lowest read number in the dataset (4,977 counts). Raw sequence data for this study was deposited at the European Nucleotide Archive (ENA) under the study accession number PRJEB44209 (<http://www.ebi.ac.uk/ena/data/view/PRJEB44209>).

## Component Balance and Estimation of O<sub>2</sub> Contamination

Assumptions and calculation steps used for the component balances in the gas recirculation reactors were described previously (Baleeiro et al., 2021b). Direct measurements of O<sub>2</sub> concentration (such as by using dissolved oxygen probes) are not adequate to monitor micro-aerobic environments (Krayzelova et al., 2015). Therefore, O<sub>2</sub> contamination was determined indirectly *via* the N<sub>2</sub> concentration in the recirculating gas, using the N<sub>2</sub>:O<sub>2</sub> ratio in air of 3.73 according to the following equation:

$$O_2 \text{ contamination rate } [mL d^{-1}] = (Y_2 V_{gas 2} - Y_1 V_{gas 1}) / [3.73 (t_2 - t_1)] \quad (1)$$

for sampling points 1 and 2:  $Y$  is the volumetric fraction of N<sub>2</sub> in the gas phase;  $V_{gas}$  is the gas volume of the system in mL; and  $t$  is the sampling time in days. Eq. 1 holds true if no N<sub>2</sub> is formed or consumed in the reactor, if O<sub>2</sub> is below the detection limit, and if the increase in the system's gas volume due to air leaking in can be neglected. Calculations of contamination rates in the control reactors (STR-control and BCR-control) were used to determine standard errors for the O<sub>2</sub> contamination rate (Supplementary Figure S1). ORP measurements did not show a clear relation with O<sub>2</sub> contamination rates (Supplementary Figure S2) and were, hence, not used to quantify rates.

## RESULTS

The experiments were divided into two periods, each with one air contamination event. STR-test and BCR-test were contaminated with O<sub>2</sub> from air for certain periods, while STR-control and BCR-control remained virtually anoxic throughout the study (calculated average contamination rates of  $7 \pm 33$  and  $3 \pm 28$  mL O<sub>2</sub> L<sup>-1</sup> d<sup>-1</sup>, respectively) and were adopted as controls for anoxic reactor operation. Before the start of each period, the broths of each reactor pair were mixed so that each pair started with a similar microbial community and broth composition. The broths from the STRs were not mixed with the broths from the

BCRs, resulting in communities developing independently for each reactor type.

## General Performance of the Gas Recirculation Reactors

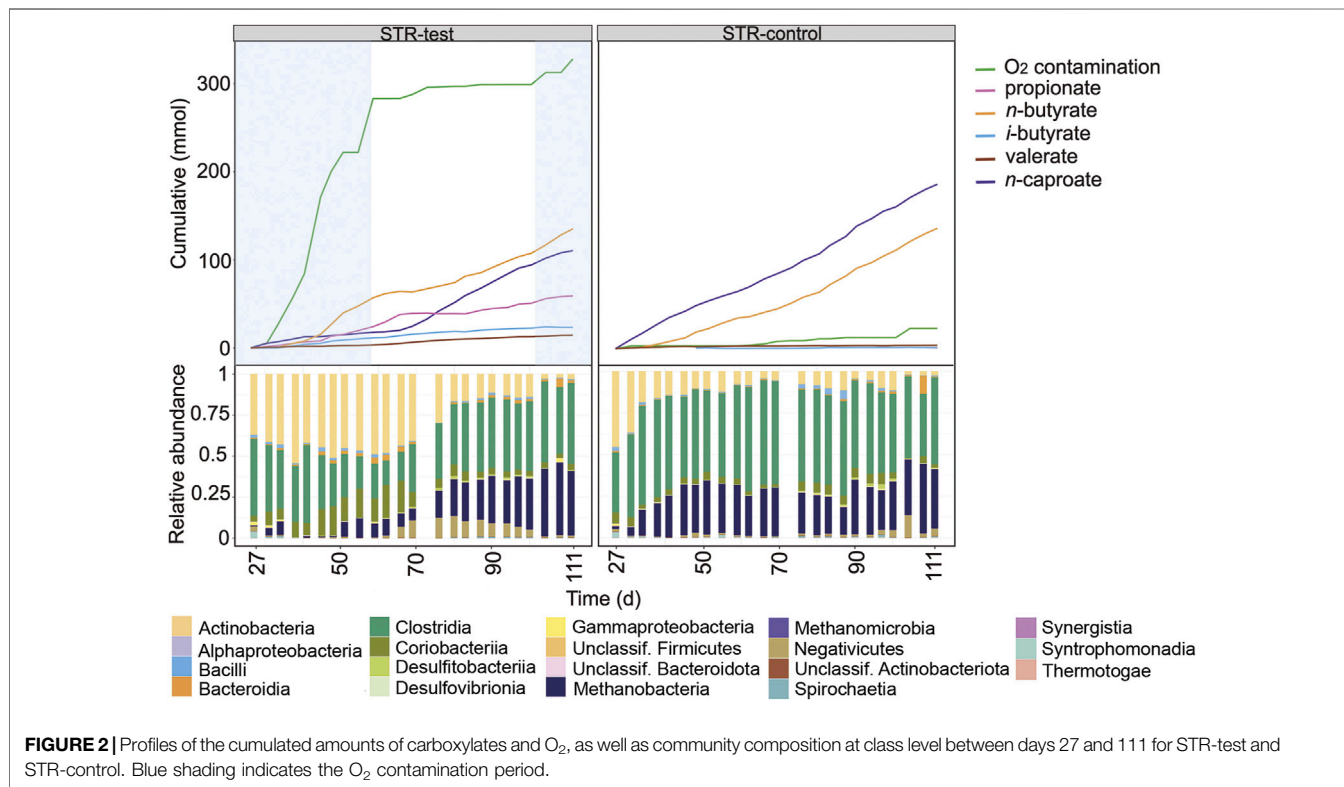
The main carboxylates produced were propionate, *n*-butyrate, *i*-butyrate, *n*-valerate, *n*-caproate, and *n*-caprylate, with maximum concentrations presented in Table 1. The STRs reached higher *n*-caproate maxima and were the only ones in which *n*-caprylate was detected, whereas the BCRs reached higher propionate, *n*-valerate, and *i*-butyrate maxima. These differences can also be seen in terms of specific production and consumption rates given in mmol L<sup>-1</sup> d<sup>-1</sup> in Supplementary Table S1. For all reactors, most of the lactate fed was consumed and differences in its consumption rates were due to washout of unconsumed substrate (Supplementary Table S1). Except for the period when O<sub>2</sub> was present in detectable amounts, net consumption of acetate occurred in all reactors, ranging from 1.4 to 4.4 mmol L<sup>-1</sup> d<sup>-1</sup>, which corresponded to a small fraction of the total acetate fed (14.3 mmol L<sup>-1</sup> d<sup>-1</sup>). With the exception of STR-control, where very little *i*-butyrate was produced, *i*-butyrate production rates ranged from 0.23 to 1.08 mmol L<sup>-1</sup> d<sup>-1</sup> and showed no clear relation to O<sub>2</sub> contamination (Supplementary Table S1).

According to previous experience with the H<sub>2</sub>/CO<sub>2</sub> recirculation reactors, ethylene was used to inhibit CH<sub>4</sub> production. Even though the partial pressure of ethylene was higher than 1 kPa at all times, methanogens gradually acclimatized to the inhibitor. Methanogenesis was observed first in the reactors that remained anoxic throughout the experimental time: in BCR-control from day 0 and in STR-control from day 31. Later on, methanogenesis was also observed in STR-test from day 48 and in BCR-test from day 60. Methane production rates were similar in the control reactors STR-control and BCR-control (16.5 and 15.9 mmol L<sup>-1</sup> d<sup>-1</sup>, respectively) and the highest rate observed over a sustained period was 19.5 mmol L<sup>-1</sup> d<sup>-1</sup> during an anoxic operation period between days 59 and 111 of STR-test (Supplementary Table S1).

With 200 mM acetate (12 g L<sup>-1</sup>) originally present in the growth medium, no net acetate formation was observed and no clear signs of homoacetogenic activity were found. After discounting the H<sub>2</sub> used for CH<sub>4</sub> formation (assuming 1 mol CH<sub>4</sub> produced from 4 mol H<sub>2</sub>), almost no additional H<sub>2</sub> consumption was seen in the control reactors STR-control and BCR-control. STR-control had a net H<sub>2</sub> formation of 3.73 mmol L<sup>-1</sup> d<sup>-1</sup>, whereas BCR-control showed a net H<sub>2</sub> consumption of 0.50 mmol L<sup>-1</sup> d<sup>-1</sup> (Supplementary Table S1). In the periods with O<sub>2</sub> contamination, H<sub>2</sub> consumption rates remained relatively high, despite low methanogenic activity. STR-test showed additional H<sub>2</sub> consumption of 26.3 mmol L<sup>-1</sup> d<sup>-1</sup> between days 27 and 59 and of 64.7 mmol L<sup>-1</sup> d<sup>-1</sup> between days 115 and 119 (Supplementary Table S1). This consumption of H<sub>2</sub> corresponded from 3.0 to 3.4 times the molar consumption of O<sub>2</sub> in the same period. In aerated periods in BCR-test, H<sub>2</sub>

**TABLE 1** | Maximum concentration of carboxylates achieved in the experiments.

Reactor	Maximum concentration (g L <sup>-1</sup> )					
	propionate	<i>n</i> -butyrate	<i>i</i> -butyrate	<i>n</i> -valerate	<i>n</i> -caproate	<i>n</i> -caprylate
STR-control	1.3	3.4	0.5	0.3	4.6	1.1
STR-test	1.7	5.7	0.6	0.4	3.5	1.0
BCR-control	2.7	4.1	2.2	1.0	3.0	—
BCR-test	3.1	4.7	1.6	0.6	3.5	—



consumption after discounting methane production ranged from 1.1 to 3.6 times the oxygen consumption.

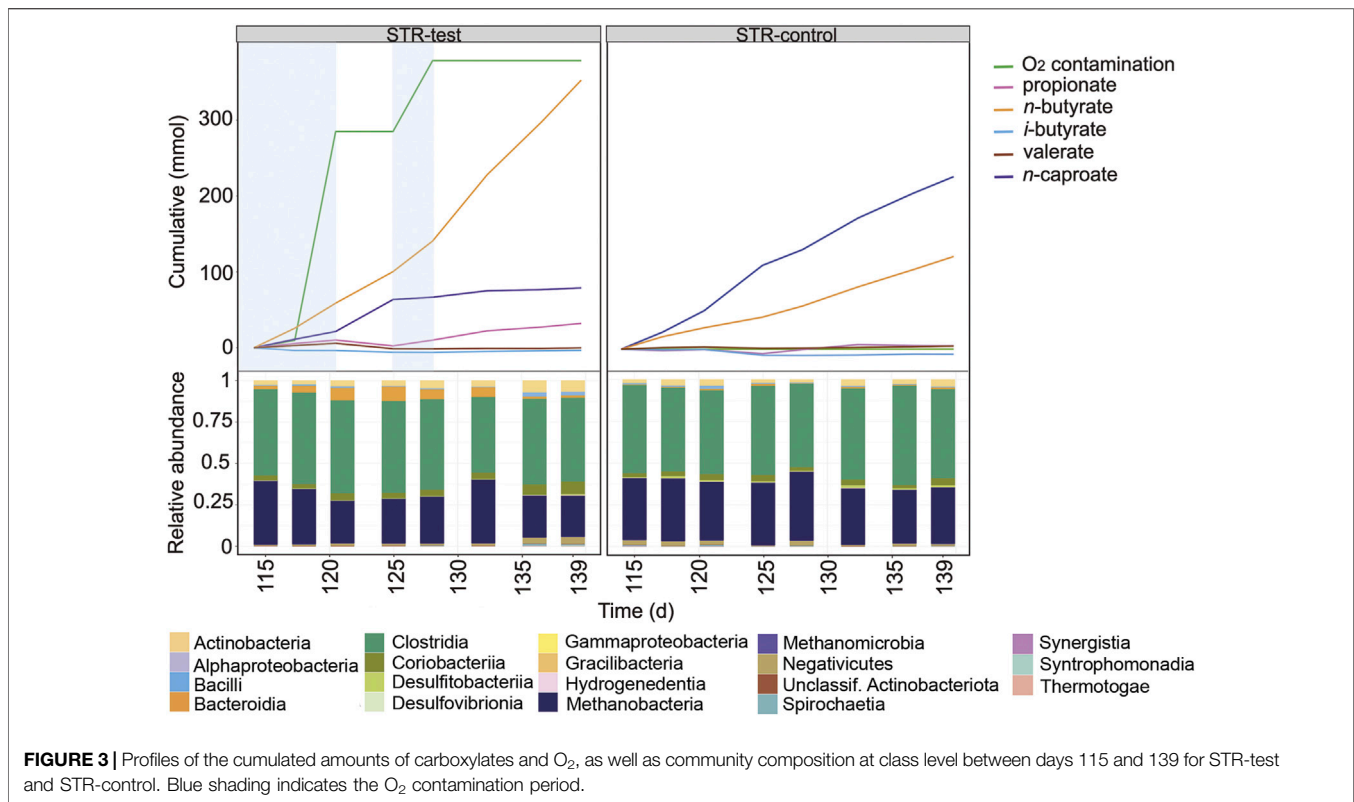
Electron balances encompassing the whole period of fermentation had errors of -0.63% (i.e., 0.63% of the monitored pool of electron equivalents had unexplained consumption) for STR-test, -0.73% for STR-control, -0.93% for BCR-control, and -1.61% for BCR-test.

## Effect of O<sub>2</sub> on the Fermentation in the Stirred Tank Reactor

Figure 2 shows the profiles of the cumulated amounts of carboxylates and O<sub>2</sub> as well as the microbial community composition at class level for the first period comparing the STRs. Between days 27 and 59, O<sub>2</sub> concentration in the gas phase remained below the detection limit in STR-test (Supplementary Figure S3), although a contamination rate of 220 ± 33 mL O<sub>2</sub> L<sup>-1</sup> d<sup>-1</sup> was detected. Between days 59 and 111, STR-test

had an anoxic operation period although small O<sub>2</sub> contaminations occurred between days 104 and 111 (Figure 2) and were the reason why the reactor could not reach perfectly anoxic conditions (21 ± 33 mL O<sub>2</sub> L<sup>-1</sup> d<sup>-1</sup>).

Even though *n*-butyrate and *n*-caproate were the main carboxylates produced in both reactors, *n*-caproate production in STR-test was, with 0.56 mmol L<sup>-1</sup> d<sup>-1</sup>, 72% lower than in STR-control (2.12 mmol L<sup>-1</sup> d<sup>-1</sup>) during the contamination period (days 27–59, Figure 2). Under O<sub>2</sub> stress, STR-test produced more propionate (0.76 mmol L<sup>-1</sup> d<sup>-1</sup>, 6.4 times that of the control) but *n*-butyrate production was similar in both reactors. Moreover, O<sub>2</sub> contamination in STR-test caused 63% less methane production (6.05 of 16.5 mmol L<sup>-1</sup> d<sup>-1</sup>) and 38% less acetate consumption (1.80 of 2.91 mmol L<sup>-1</sup> d<sup>-1</sup>, Supplementary Table S1). After anoxic conditions in STR-test had been restored (days 59–111), methane production was 18% higher than in the control reactor (19.5 of 16.5 mmol L<sup>-1</sup> d<sup>-1</sup>) and propionate production decreased slightly to 0.67 mmol L<sup>-1</sup> d<sup>-1</sup>.



Under anoxic conditions in STR-test, propionate production slowed down from day 66 on, coinciding with an acceleration of *n*-caproate production (Figure 2), which was still 16% lower than in the control (1.78 of 2.12 mmol L<sup>-1</sup> d<sup>-1</sup>).

O<sub>2</sub> contamination caused differences in microbial community composition that were visible up to the class level (Figure 2). Clostridia and Methanobacteria predominated in the reactor that remained completely anoxic. In the other reactor, Actinobacteria and Coriobacteriia were the main classes found in periods when O<sub>2</sub> contamination occurred. The community of STR-test converged to a composition similar to that of the control reactor after anoxic conditions had been restored.

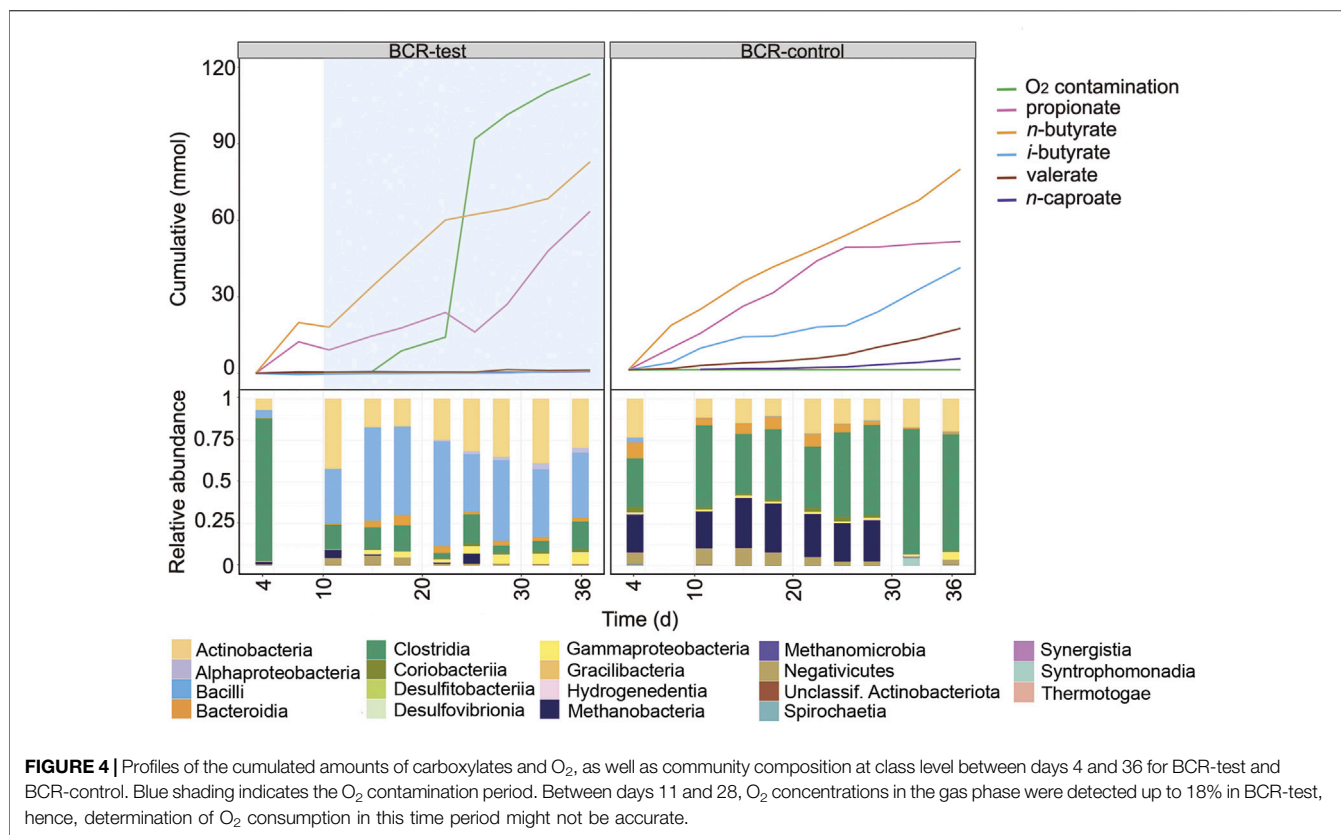
For the same operation period, community composition with resolution to the genus level and concentrations of the main carboxylates are shown in Supplementary Figure S4. Clostridia were mainly represented by the genera *Caproiciproducens*, *Clostridium sensu stricto* 12, and *Oscillibacter*, while the Actinobacteria belonged to the genera *Acidipropionibacterium* and *Actinomyces*. Methanogens were from the genus *Methanobrevibacter* and the Coriobacteriia were from the family *Eggerthellaceae*.

A second O<sub>2</sub> contamination event occurred in STR-test between days 115 and 119 (Figure 3), this time for a shorter period but at double rate (471 ± 33 mL O<sub>2</sub> L<sup>-1</sup> d<sup>-1</sup>) (Supplementary Table S1). With the new contamination event in STR-test, CH<sub>4</sub> and *n*-caproate production rates fell to 32% (5.33 of 16.5 mmol L<sup>-1</sup> d<sup>-1</sup>) and 50% (1.06 of 2.12 mmol L<sup>-1</sup> d<sup>-1</sup>) of those of the control reactor, respectively (Supplementary Table S1). This time, the O<sub>2</sub> contamination

coincided with an increase in *n*-butyrate formation rate from 1.51 to 2.76 mmol L<sup>-1</sup> d<sup>-1</sup>, and instead of increasing propionate production, *n*-valerate production reached four times that of the control reactor (0.29 in relation to 0.07 mmol L<sup>-1</sup> d<sup>-1</sup>). The short period of intense O<sub>2</sub> contamination had a smaller impact on the microbial community composition and coincided with an increase in relative abundance of *Prevotella* belonging to the Bacteroidia (Supplementary Figure S5). In the last 20 days of operation of STR-test, O<sub>2</sub> contamination was reduced but not completely stopped (39 ± 33 mL O<sub>2</sub> L<sup>-1</sup> d<sup>-1</sup>, Supplementary Table S1) as shown between days 125 and 128 (Figure 3). In this period, propionate production decreased to its lowest value in STR-test and *n*-butyrate production increased once more to 4.77 mmol L<sup>-1</sup> d<sup>-1</sup>. Although CH<sub>4</sub> formation increased again to the level observed during anoxic operation, *n*-caproate production could not be restored (Figure 3).

## Effect of O<sub>2</sub> on the Fermentation in the Bubble Column Reactor

The earlier operation phase of the BCRs is shown in Figure 4 and in Supplementary Figure S6. For this comparison period, the mixing of broths was not enough to ensure equal community compositions in BCR-test and BCR-control. The O<sub>2</sub> contamination period between days 11 and 36 in BCR-test differed from the other contamination events since O<sub>2</sub> concentrations up to 18% were detected in the gas phase between days 11 and 28 (Supplementary Figure S3). Considering that the assumptions for balance calculations in



the reactors do not account for high O<sub>2</sub> concentrations, the O<sub>2</sub> contamination rate determined for this period ( $97 \pm 28 \text{ mL O}_2 \text{ L}^{-1} \text{ d}^{-1}$ ) might be inaccurate. When O<sub>2</sub> was detected in the system, the microbial community in the BCR-test showed a strong dominance of *Rummeliibacillus* (Supplementary Figure S6) accompanied by Actinobacteria and Gammaproteobacteria (Figure 4).

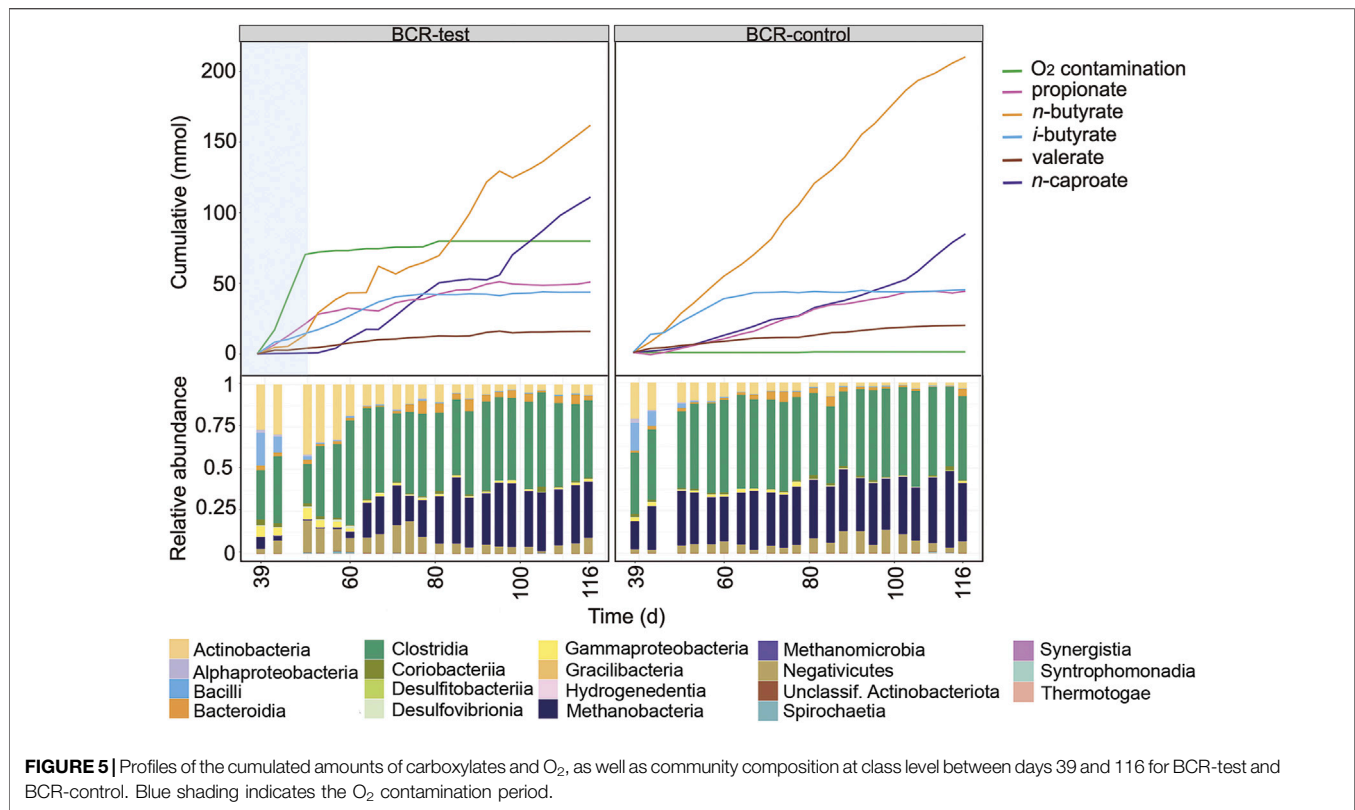
After mixing the broths of the bubble columns to start a new comparison period, BCR-test received  $129 \pm 28 \text{ mL O}_2 \text{ L}^{-1} \text{ d}^{-1}$  between days 39 and 50 whereas BCR-control remained completely anoxic (Figure 5). During the contamination period, BCR-test produced virtually no *n*-caproate ( $0.03 \text{ mmol L}^{-1} \text{ d}^{-1}$  in comparison to  $0.92 \text{ mmol L}^{-1} \text{ d}^{-1}$  in control) and propionate was produced instead ( $1.78 \text{ mmol L}^{-1} \text{ d}^{-1}$ , 2.8 times that of the control). With O<sub>2</sub> contamination, BCR-test produced 46% less *n*-butyrate ( $1.22$  of  $2.25 \text{ mmol L}^{-1} \text{ d}^{-1}$ ) and 91% less methane ( $1.41$  of  $15.9 \text{ mmol L}^{-1} \text{ d}^{-1}$ ) than the control (Supplementary Table S1). After O<sub>2</sub> contamination stopped in BCR-test (from day 50 on), *n*-caproate production recovered with a rate of  $1.40 \text{ mmol L}^{-1} \text{ d}^{-1}$  while propionate formation decreased to  $0.34 \text{ mmol L}^{-1} \text{ d}^{-1}$ . *n*-Butyrate and methane production recovered partially and remained 18% ( $1.84$  of  $2.25 \text{ mmol L}^{-1} \text{ d}^{-1}$ ) and 25% ( $11.9$  of  $15.9 \text{ mmol L}^{-1} \text{ d}^{-1}$ ) lower than that of the control, respectively.

Similarly to what was seen in the STRs, Actinobacteria increased their relative abundances at the cost of Clostridia and Methanobacteria during the O<sub>2</sub> contamination period in

BCR-test (Figure 5). In addition, Gammaproteobacteria also became more abundant during the contamination. Visualization of the community development at genus level in Supplementary Figure S7 reveals that the main genera of Actinobacteria were the same as those found in the STRs (i.e., *Acidipropionibacterium* and *Actinomyces*). Besides the Clostridia genera that dominated in the STRs, a transient presence of *Eubacterium* was also observed in the BCRs. Gammaproteobacteria were represented by *Sutterella* and *Burkholderia* (Supplementary Figure S7).

## Correlations between Community Members and Abiotic Parameters

Figure 6 shows Spearman correlations between the most abundant genera, O<sub>2</sub> contamination, and the formation or consumption rates of the main chemicals. In Supplementary Table S2, the correlation coefficients and their *p*-values are listed. Positive correlations of *n*-caproate formation and relative abundances of *Caproiciproducens*, unclassified *Peptostreptococcales*, and *Methanobrevibacter* were found, whereas *Clostridium sensu stricto* 12, unclassified *Micrococcales*, *Acidipropionibacterium*, *Burkholderia*, *Rummeliibacillus*, *Dialister*, and *Sutterella* correlated negatively. Propionate production correlated positively to abundances of *Acidipropionibacterium*, *Burkholderia*, and *Proteiniphilum*. O<sub>2</sub> contamination correlated negatively with *Methanobrevibacter*, whereas positive correlations were found with abundances of



unclassified *Eggerthellaceae*, unclassified *Actinomycetaceae*, *Actinomyces*, and *Proteiniphilum*. Abundances of *Clostridium sensu stricto* 12, *Acidipropionibacterium*, *Acidaminococcus*, and *Dialister* correlated positively with *i*-butyrate and *n*-valerate production. H<sub>2</sub> consumption after discounting methane production (i.e. non-CH<sub>4</sub> H<sub>2</sub> consumption) correlated positively with *Acidipropionibacterium*, *Actinomyces*, and unclassified *Micrococcales*. *i*-Butyrate production correlated negatively with relative abundances of *Methanobrevibacter*, *Caproiciproducens*, and unclassified *Peptostreptococcales*.

Among the most abundant amplicon sequence variants (ASVs), *Clostridium sensu stricto* 12 and *Acidipropionibacterium* had ASVs that were identical to isolated species in the Silva 138 database. Within the genus *Clostridium sensu stricto* 12, ASVs were assigned to *C. luticellarii*, *C. tyrobutyricum*, or *C. ljungdahlii* (the latter was also ambiguously assigned to *C. autoethanogenum*, *C. ragsdalei*, and *C. coskatii*). ASVs within *Acidipropionibacterium* were assigned to *A. acidipropionici*.

## DISCUSSION

Regardless of O<sub>2</sub> contamination, the BCRs had higher concentrations of propionate, *i*-butyrate, and *n*-valerate, whereas the stirred tank design facilitated higher concentrations of *n*-butyrate, *n*-caproate, and *n*-caprylate (Table 1). The production of *n*-valerate and *i*-butyrate was not clearly related to O<sub>2</sub> contamination (Figures 2, 5 and

Supplementary Table S1), but its connection to *Clostridium sensu stricto* 12 (Figure 6), specifically *C. luticellarii*, was observed previously (de Smit et al., 2019; de Leeuw et al., 2020; Huang et al., 2020; Baleeiro et al., 2021a). *C. luticellarii* was shown to be important for *n*-valerate production from propionate (de Smit et al., 2019) and could therefore play an important role in the production of odd-chain MCC in chain elongation reactors. *n*-Valerate and *i*-butyrate production also correlated with other genera that are not commonly known for the production of these compounds (Figure 6). Higher relative abundances of *Caproiciproducens* not only correlated significantly with *n*-caproate production (Figure 6) but were visually related to higher concentrations of *n*-caproate (Supplementary Figures S4, S7). The correlation of *n*-caproate production with the abundance of *Caproiciproducens* is not surprising, since this genus has been commonly found in other MCC-producing communities (Duber et al., 2020; Joshi et al., 2021).

Micro-aerobic conditions favored the classes Actinobacteria, Gammaproteobacteria, Bacilli, and Coriobacteriia over Clostridia and Methanobacteria. Notably, a similar pattern is known for gut microbiota, where Actinobacteria and Alpha- or Gammaproteobacteria have been observed to dominate over Clostridia in regions of the gut more exposed to O<sub>2</sub> (Friedman et al., 2018). One explanation is that the evolutionary younger taxa of aerotolerant Actinobacteria (e.g., propionibacteria) and Proteobacteria (Martin and Sousa, 2015) are generally better equipped with enzymes that mitigate the toxicity of ROS (e.g., catalases, H<sub>2</sub>O<sub>2</sub> reductases, and superoxide dismutases) than



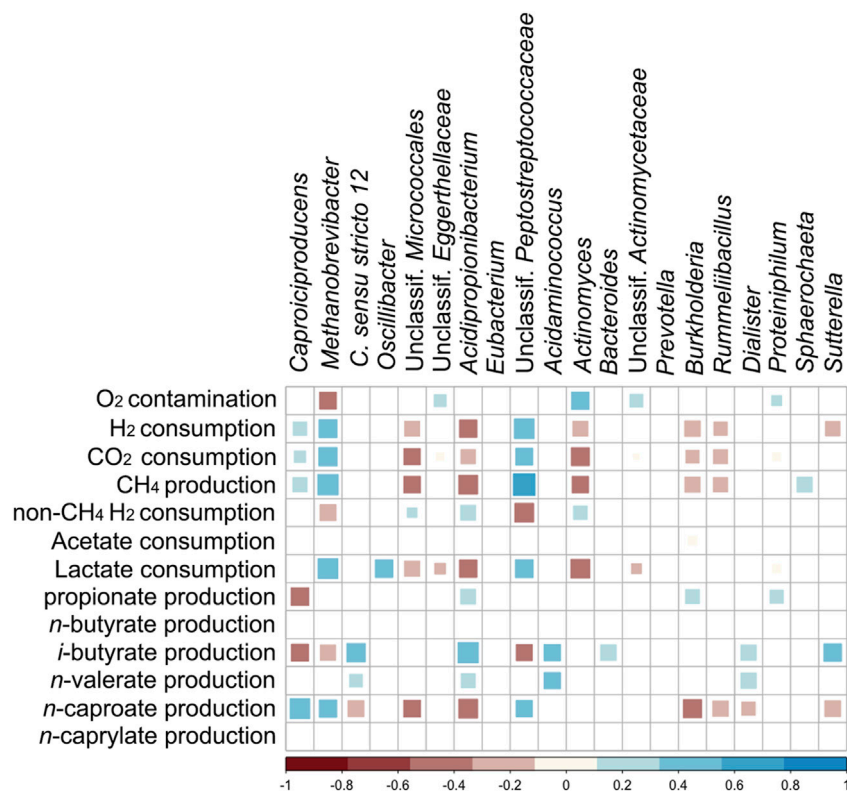


**FIGURE 6** | Spearman correlation matrix between the most abundant genera, O<sub>2</sub> contamination rate, and production/consumption rates of chemicals ( $p < 0.01$ ). "non-CH<sub>4</sub> H<sub>2</sub> consumption" stands for H<sub>2</sub> consumption after discounting methane formation.

typical strict anaerobes such as Clostridia (Kato et al., 1997; Johnson and Hug, 2019).

## Partial Acclimatization of Methanogens to Ethylene

Hydrogenotrophic methanogenesis was likely the main pathway for CH<sub>4</sub> production. This is supported by the results of previous experiments where *Methanobrevibacter* was one of the predominating community members under similar conditions with H<sub>2</sub>/CO<sub>2</sub> (Baleeiro et al., 2021a). Notably, methanogens partially overcame the inhibition by ethylene. The acclimatization occurred after 42 days of successful inhibition reported by Baleeiro et al. (2021b). To the best of our knowledge, such acclimatization has not been reported before. With ethylene, CH<sub>4</sub> production was relatively strong (up to 19.5 mmol L<sup>-1</sup> d<sup>-1</sup>) but still about one third lower than the rates observed in the absence of the inhibitor in a similar gas recirculation system (up to 32.8 mmol L<sup>-1</sup> d<sup>-1</sup>) (Baleeiro et al., 2021b). We hypothesize that *Methanobrevibacter*, the main methanogenic genus found in our reactors, may have acclimatized to ethylene by expressing [Fe]-hydrogenases. For hydrogenotrophic methanogens, [Fe]-hydrogenases have less favorable kinetics than [NiFe]-hydrogenases. Still, some methanogens, including Methanobacteria, can express [Fe]-hydrogenases to grow under nickel-limiting conditions (Thauer et al., 2010). As

postulated by Baleeiro et al. (2021b), ethylene might not exert an inhibitory effect on nickel-free hydrogenases as it does on [NiFe]-hydrogenases of methanogens. Considering that [Fe]-hydrogenases are not inhibited by O<sub>2</sub> (Thauer et al., 2010; Stiebritz and Reiher, 2012), micro-aerobic conditions and broth mixing between reactors could have caused further selection of methanogens expressing [Fe]-hydrogenases even if nickel was not limiting. Further studies using transcriptome or proteome analyses of pure methanogenic cultures are needed to test this hypothesis.

## Steering the Fermentation with Small O<sub>2</sub> Contamination

When the O<sub>2</sub> concentration in the gas phase increased up to 18% between days 11 and 28, the aerobic genus *Rummeliibacillus* (Vaishampayan et al., 2009; Her and Kim, 2013) flourished in the bubble column reactor and the concentrations of *n*-butyrate and propionate decreased (**Supplementary Figure S6**). With an O<sub>2</sub> concentration below the detection limit by day 28 (**Supplementary Figure S3**), Actinobacteria abundance increased and propionate production reached its highest rates (**Supplementary Table S1**).

Methanogenesis and *n*-caproate production were strongly inhibited by O<sub>2</sub> intrusion. After the contamination stopped, CH<sub>4</sub> production recovered on every occasion but *n*-caproate

production did not (**Supplementary Table S1**), indicating that the O<sub>2</sub> contamination had particularly strong detrimental effects on C4-to-C6 chain elongation. In the period between days 119 and 139 in STR-test, *n*-caproate production did not increase after O<sub>2</sub> contamination rate changed from 474 ± 33 mL O<sub>2</sub> L<sup>-1</sup> d<sup>-1</sup> to 39 ± 33 mL O<sub>2</sub> L<sup>-1</sup> d<sup>-1</sup>, instead, the highest rates of *n*-butyrate production and acetate consumption were achieved. This was observed even with high relative abundances of *Caproiciproducens* in the community (**Supplementary Figure S5**).

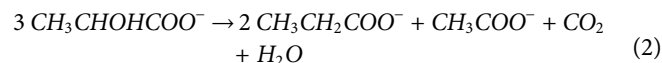
Relatively low O<sub>2</sub> contamination rates were found to favor propionate formation in lactate-based fermentation. However, the relationship between O<sub>2</sub> and propionate accumulation was not as straightforward as the inhibitory effect of O<sub>2</sub> on chain elongation and methanogenesis. One possible reason is that propionate is not only a product of lactate fermentation, but also a substrate for *n*-valerate production by chain-elongating bacteria (Angenent et al., 2016). This could explain what was observed in the micro-aerobic period between days 115 and 119 in the STR-test, when propionate production did not increase but *n*-valerate production was relatively high (**Supplementary Table S1**).

### Key Players that can Profit from O<sub>2</sub> Intrusion

Among the microorganisms enriched in the O<sub>2</sub> contamination periods, *Acidipropionibacterium* correlated to propionate production ( $p < 0.01$ ). Other Actinobacteria enriched during O<sub>2</sub> contamination did not correlate with propionate production and may have diverted electrons from lactate to products other than propionate, which could be another reason why STR-test showed lower propionate production rates (**Supplementary Table S1**). *Actinomyces*, a facultative anaerobe (Rao et al., 2012), was particularly enriched in STR-test during an O<sub>2</sub> contamination period (**Supplementary Figure S4**). *Actinomyces* can grow anaerobically or aerobically on lactate and produces acetate, formate, and CO<sub>2</sub> during fermentative growth (Takahashi et al., 1994; Takahashi and Yamada, 1999; Rao et al., 2012). In agreement with the reported aerobic growth of *Actinomyces naeslundii* on lactate (Takahashi and Yamada, 1999), *Actinomyces* was likely not responsible for propionate production in the STR. The Coriobacteria (*Eggerthellaceae*) observed in O<sub>2</sub> contamination periods belong to a family of strict anaerobes that are not reported to produce propionate (Gupta et al., 2013). *Proteiniphilum* (as well as *Dialister*) are genera with microaerophilic species that produce propionate, although it is not clear if from lactate (Tomazetto et al., 2018; Sakamoto et al., 2020). In our study, the abundance of *Proteiniphilum* correlated to O<sub>2</sub> contamination and to propionate formation whereas no significant correlation was found between *Dialister*, propionate, and O<sub>2</sub> contamination (**Figure 6**).

Fermentation of lactate by propionate producing bacteria commonly leads to a 2:1:1 stoichiometry of propionate to acetate to CO<sub>2</sub> (**Eq. 2**). Gammaproteobacteria and Actinobacteria species that produce propionate are known to use methylmalonyl-CoA pathways rather than the acrylate pathway (Seeliger et al., 2002; Gonzalez-Garcia

et al., 2017). In particular, *Acidipropionibacterium* spp. are among the most efficient propionate producers thanks to the highest energy efficiency of their methylmalonyl-CoA pathway (also known as Wood-Werkman cycle, a succinate pathway involving methylmalonyl-CoA:pyruvate transcarboxylase) (Scholz and Kilian, 2016; Gonzalez-Garcia et al., 2017).



Even though it can express O<sub>2</sub>-sensitive enzymes for fermentative growth similar to those in *Clostridium*, *Acidipropionibacterium* also has aerotolerant enzymes with similar functions (Piwowarek et al., 2018; McCubbin et al., 2020). Members of this genus are not only more tolerant to O<sub>2</sub> than clostridia, they have also been found to increase propionate and energy yields when exposed to O<sub>2</sub> (McCubbin et al., 2020).

It should be taken into account that propionibacteria, unlike many clostridia, do not form endospores (Gonzalez-Garcia et al., 2017). Hence, if exploration of propionate production is desired, shock treatments of the inoculum (e.g., with pH or heat), common techniques for starting non-methanogenic anaerobic bioprocesses (Baleeiro et al., 2019), should be avoided.

The phenomenon that lactate is diverted to propionate in chain elongation reactors under micro-aerobic conditions may have been overlooked in former studies. In one notable case, Kucek et al. (2016) observed the competitive production of propionate in a lactate-based chain elongation reactor. Although the possibility of O<sub>2</sub> contamination was not discussed, the study detected high abundances of *Acinetobacter*, strictly aerobic Gammaproteobacteria (Smet et al., 2014) commonly found in micro-aerated reactors (Krayzelova et al., 2015). To explain the propionate production observed in certain time periods, Kucek et al. (2016) suggested the residual concentration of lactate in the reactor to be a determining factor. Although not discussed in the study, O<sub>2</sub> presence could have played a role in propionate production.

### Possible Roles of H<sub>2</sub> during O<sub>2</sub> Contamination

A common way for the reduction of O<sub>2</sub> in the presence of H<sub>2</sub> is shown in **Eq. 3** and is realized even by obligate anaerobes such as methanogens (Thauer et al., 2010), Negativicutes (Boga et al., 2007), and sulfate reducers (Dannenberget al., 1992; Chen et al., 1993).



H<sub>2</sub> consumption that was not attributed to methane formation was particularly high during O<sub>2</sub> contamination periods. In STR-test, it ranged from 3.0 to 3.4 fold molar O<sub>2</sub> consumption, while in BCR-test it ranged from 1.1 to 3.6 fold. Considering the 2:1 ratio of H<sub>2</sub> to O<sub>2</sub> during H<sub>2</sub> oxidation (**Eq. 3**), H<sub>2</sub> consumption not linked to methane formation in this study may have been related to other reactions during O<sub>2</sub> intrusion. Interestingly, similar

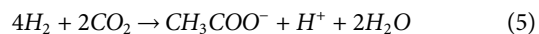
consumption ratios of H<sub>2</sub> to O<sub>2</sub> (between 3.2 and 3.4) have been observed in communities dominated by hydrogen-oxidizing bacteria during autotrophic growth (Matassa et al., 2016). Nevertheless, we did not observe the presence of *Sulfuricurvum* (the genus enriched by Matassa et al. (2016)) and *Burkholderia*, a possible aerobic autotroph (Takors et al., 2018) found in our study, did not correlate positively with H<sub>2</sub> consumption nor with O<sub>2</sub> contamination. Besides, if aerobic hydrogen-oxidizing bacteria played a major role in the micro-aerobic reactors in our study, signs of biomass formation and carbon source (e.g., CO<sub>2</sub>) consumption should have accompanied H<sub>2</sub> oxidation with O<sub>2</sub>. However, no clear relation between O<sub>2</sub> contamination, biomass formation, and CO<sub>2</sub> consumption rates was found.

Communities enriched with propionate-producing bacteria in anaerobic reactors, such as *Acidipropionibacterium* spp., often correlate with high H<sub>2</sub> consumption or low H<sub>2</sub> production (Cabrol et al., 2017). In the presence of exogenous H<sub>2</sub>, some propionate producers such as *Propionispira arboris* are able to perform homopropionate fermentation of lactate (Eq. 4) producing neither CO<sub>2</sub> nor acetate (Thompson et al., 1984).



We did not observe *Propionispira* spp. in our reactors and its closest relative found in our system (*Dialister*) is only related at the order level (*Veillonellales-Selenomonadales*). Besides, Eq. 4 alone cannot explain the high H<sub>2</sub> consumption during most of the micro-aerobic periods in this study. H<sub>2</sub> consumption not linked to methane was much higher than propionate formation. In fact, the period between days 39 and 50 of BCR-test had the lowest H<sub>2</sub> to O<sub>2</sub> consumption ratio and was the period with the highest propionate productivity (Supplementary Table S1). Lastly, it is not clear if the correlation found between abundance of *Acidipropionibacterium* and H<sub>2</sub> consumption not linked to methane (Figure 6) is a direct one. H<sub>2</sub> consumption by isolated members of *Propionibacterium* is not observed during fermentative growth (Seeliger et al., 2002).

Homoacetogens consume H<sub>2</sub> and CO<sub>2</sub> (Eq. 5) and, among them, at least *C. ljungdahlii* was shown to have some resistance against O<sub>2</sub> exposure (Whitham et al., 2015). Here, similar clostridia were detected in the reactors and *Clostridium sensu stricto* 12 was still present during some O<sub>2</sub> contamination events (Supplementary Figures S3, S7). Therefore, homoacetogenic activity could be considered to explain H<sub>2</sub> consumption during O<sub>2</sub> contamination. Nevertheless, no further evidence for this hypothesis was found. H<sub>2</sub> consumption was not accompanied by net CO<sub>2</sub> consumption and the net acetate production was unfavorable because acetate was fed in excess with the growth medium (12 g L<sup>-1</sup> acetate) to favor chain elongation as an acetate-consuming reaction.



Another way that H<sub>2</sub> presence might have influenced the micro-aerated community is by amplifying the effects of O<sub>2</sub> contamination. The activation of O<sub>2</sub> into ROS by hydrogenases and reduced electron carriers might be accentuated by H<sub>2</sub> recirculation (Misra and Fridovich, 1971; Krab et al., 1982). Since we did not have a control reactor for the presence of H<sub>2</sub>, we could not test this hypothesis.

## CONCLUSION

Even small O<sub>2</sub> contaminations were very detrimental to *n*-caproate and methane formation, but favored propionate formation. The relation of O<sub>2</sub> contamination and propionate formation was not straightforward: reactors with micro-aerobic conditions produced more propionate overall, but propionate production cycles were not always synchronous to O<sub>2</sub> contamination. Besides, the negative effects of O<sub>2</sub> on methane formation could be reversed in all cases whereas chain elongation could not always be resumed when O<sub>2</sub> contamination stopped. These patterns were observed in both stirred tank and in bubble column reactors, with the bubble column process being more sensitive to O<sub>2</sub> contamination.

It is unclear whether the effects of O<sub>2</sub> reported in this study could be reproduced without the recirculation of H<sub>2</sub>. It is possible that the H<sub>2</sub> recirculation amplified the effects of O<sub>2</sub> toxicity, since presence of H<sub>2</sub> can favor ROS formation by hydrogenases. Considering that H<sub>2</sub> consumption was particularly high during micro-aeration, H<sub>2</sub> may have acted as an important energy source for aerotolerant and aerobic microorganisms. Controlled O<sub>2</sub> contamination studies with co-cultures or mixed communities of lower complexity can shed light on how impactful H<sub>2</sub> recirculation during micro-aeration is.

Aerotolerant fermenting bacteria such as *Acidipropionibacterium* spp. are efficient propionate producers that could be regarded as welcomed guests rather than competitors. Here, they were the main candidates responsible for propionate production although their correlation with O<sub>2</sub> contamination was unclear. Instead, *Actinomyces* spp. (Actinobacteria that did not produce propionate) profited most from the micro-aerobic environment. Future experiments could help clarify if stable propionate-producing communities can be selected by micro-aeration. If micro-aeration facilitates propionate accumulation, a sequential anaerobic step can be used for chain elongation with high selectivity to odd-numbered MCC. Studies with defined cultures aiming to understand what is behind the recovery of chain elongation activity after micro-aerobic periods are also recommended.

## DATA AVAILABILITY STATEMENT

The datasets generated for this study can be found in the European Nucleotide Archive (ENA) under accession number PRJEB44209 (<http://www.ebi.ac.uk/ena/data/view/PRJEB44209>).

## AUTHOR CONTRIBUTIONS

Conceptualization: FB and HS; methodology: FB; investigation: FB and MA; formal analysis, data curation, and visualization: FB and MA; writing (original draft preparation): FB and MA; writing (review and editing): FB, MA, SK, and HS; supervision: SK and HS; project administration: SK and HS. All authors have read and agreed to the published version of the manuscript.

## FUNDING

This study was funded by the Helmholtz Association, Research Program Renewable Energies. Financial support was also received from the CAPES–Brazilian Federal Agency for Support and Evaluation of Graduate Education within the Ministry of Education of Brazil (No. 88887.163504/2018–00) and from the

## REFERENCES

- Andersen, S. J., De Groof, V., Khor, W. C., Roume, H., Props, R., Coma, M., et al. (2017). A *Clostridium* Group IV Species Dominates and Suppresses a Mixed Culture Fermentation by Tolerance to Medium Chain Fatty Acids Products. *Front. Bioeng. Biotechnol.* 5, 8. doi:10.3389/fbioe.2017.00008
- Angenent, L. T., Richter, H., Buckel, W., Spirito, C. M., Steinbusch, K. J. J., Plugge, C. M., et al. (2016). Chain Elongation with Reactor Microbiomes: Open-Culture Biotechnology to Produce Biochemicals. *Environ. Sci. Technol.* 50 (6), 2796–2810. doi:10.1021/acs.est.5b04847
- Apelt, M. (2020). “Examination of Samples of Solids (Substrates) and Digestates with HPLC for Aliphatic and Aromatic Acids, Alcohols and Aldehydes,” in *Series “Biomass Energy Use”: Collection of Methods for Biogas: Methods to Determine Parameters for Analysis Purposes and Parameters that Describe Processes in the Biogas Sector*. Editors J. Liebetrau, D. Pfeiffer, and D. Thrän. 2nd ed (Leipzig: DBFZ).
- Baleeiro, F. C. F., Kleinstüber, S., Neumann, A., and Sträuber, H. (2019). Syngas-aided Anaerobic Fermentation for Medium-Chain Carboxylate and Alcohol Production: the Case for Microbial Communities. *Appl. Microbiol. Biotechnol.* 103 (21–22), 8689–8709. doi:10.1007/s00253-019-10086-9
- Baleeiro, F. C. F., Kleinstüber, S., and Sträuber, H. (2021a). Hydrogen as a Co-electron Donor for Chain Elongation with Complex Communities. *Front. Bioeng. Biotechnol.* 9, 650631. doi:10.3389/fbioe.2021.650631
- Baleeiro, F. C. F., Kleinstüber, S., and Sträuber, H. (2021b). Recirculation of H<sub>2</sub>, CO<sub>2</sub>, and Ethylene Improves Carbon Fixation and Carboxylate Yields in Anaerobic Fermentation. *bioRxiv*. 2006.2011.448067. doi:10.1101/2021.06.11.448067
- Boga, H. I., Ji, R., Ludwig, W., and Brune, A. (2006). *Sporotalea propionica* gen. nov. and sp. nov., a Hydrogen-Oxidizing, Oxygen-Reducing, Propionigenic Firmicute from the Intestinal Tract of a Soil-Feeding Termite. *Arch. Microbiol.* 187 (1), 15–27. doi:10.1007/s00203-006-0168-7
- Botheju, D., and Bakke, R. (2011). Oxygen Effects in Anaerobic Digestion - A Review. *Towmj* 4 (4), 1–19. doi:10.2174/1876400201104010001
- Cabrol, L., Marone, A., Tapia-Venegas, E., Steyer, J.-P., Ruiz-Filippi, G., and Trably, E. (2017). Microbial Ecology of Fermentative Hydrogen Producing Bioprocesses: Useful Insights for Driving the Ecosystem Function. *FEMS Microbiol. Rev.* 41 (2), 158–181. doi:10.1093/femsre/fuw043
- Chen, L., Liu, M. Y., Legall, J., Fareira, P., Santos, H., and Xavier, A. V. (1993). Rubredoxin Oxidase, a New Flavo-Hemo-Protein, Is the Site of Oxygen Reduction to Water by the “Strict Anaerobe” *Desulfovibrio gigas*. *Biochem. Biophys. Res. Commun.* 193 (1), 100–105. doi:10.1006/bbrc.1993.1595
- Dannenberg, S., Kroder, M., Dilling, W., and Cypionka, H. (1992). Oxidation of H<sub>2</sub>, Organic Compounds and Inorganic Sulfur Compounds Coupled to Reduction of O<sub>2</sub> or Nitrate by Sulfate-Reducing Bacteria. *Arch. Microbiol.* 158 (2), 93–99. doi:10.1007/BF00245211

BMBF - German Federal Ministry of Education and Research (No. 01DQ17016).

## ACKNOWLEDGMENTS

We thank Ute Lohse for technical assistance in library preparation for MiSeq amplicon sequencing and the DBFZ Department Biorefineries is acknowledged for providing the stirred tank reactors.

## SUPPLEMENTARY MATERIAL

The Supplementary Material for this article can be found online at: <https://www.frontiersin.org/articles/10.3389/fbioe.2021.725443/full#supplementary-material>

- De Groof, V., Coma, M., Arnot, T., Leak, D. J., and Lanham, A. B. (2019). Medium Chain Carboxylic Acids from Complex Organic Feedstocks by Mixed Culture Fermentation. *Molecules* 24 (3), 398. doi:10.3390/molecules24030398
- de Leeuw, K. D., de Smit, S. M., van Oossanen, S., Moerland, M. J., Buisman, C. J. N., and Strik, D. P. B. T. B. (2020). Methanol-Based Chain Elongation with Acetate to *n*-Butyrate and Isobutyrate at Varying Selectivities Dependent on pH. *ACS Sustain. Chem. Eng.* 8 (22), 8184–8194. doi:10.1021/acscuschemeng.0c00907
- de Smit, S. M., de Leeuw, K. D., Buisman, C. J. N., and Strik, D. P. B. T. B. (2019). Continuous *n*-Valerate Formation from Propionate and Methanol in an Anaerobic Chain Elongation Open-Culture Bioreactor. *Biotechnol. Biofuels* 12, 132. doi:10.1186/s13068-019-1468-x
- Duber, A., Zagrodnik, R., Chwialkowska, J., Juzwa, W., and Oleskowicz-Popiel, P. (2020). Evaluation of the Feed Composition for an Effective Medium Chain Carboxylic Acid Production in an Open Culture Fermentation. *Sci. Total Environ.* 728, 138814. doi:10.1016/j.scitotenv.2020.138814
- Friedman, E. S., Bittinger, K., Esipova, T. V., Hou, L., Chau, L., Jiang, J., et al. (2018). Microbes vs. Chemistry in the Origin of the Anaerobic Gut Lumen. *Proc. Natl. Acad. Sci. USA* 115 (16), 4170–4175. doi:10.1073/pnas.1718635115
- Giroto, F., Peng, W., Rafieenia, R., and Cossu, R. (2016). Effect of Aeration Applied during Different Phases of Anaerobic Digestion. *Waste Biomass Valor.* 9 (2), 161–174. doi:10.1007/s12649-016-9785-9
- Gonzalez-Garcia, R., McCubbin, T., Navone, L., Stowers, C., Nielsen, L., and Marcellin, E. (2017). Microbial Propionic Acid Production. *Fermentation* 3 (2), 21. doi:10.3390/fermentation3020021
- Gupta, R. S., Chen, W. J., Adeolu, M., and Chai, Y. (2013). Molecular Signatures for the Class *Coriobacteriia* and its Different Clades; Proposal for Division of the Class *Coriobacteriia* into the Emended Order *Coriobacteriales* Containing the Emended Family *Coriobacteriaceae* and *Atopobiaceae* fam. nov., and *Eggerthellales* ord. nov., Containing the Family *Eggerthellaceae* fam. nov. *Int. J. Syst. Evol. Microbiol.* 63 (Pt 9), 3379–3397. doi:10.1099/ijs.0.048371-0
- Her, J., and Kim, J. (2013). *Rummeliibacillus suwonensis* sp. nov., Isolated from Soil Collected in a Mountain Area of South Korea. *J. Microbiol.* 51 (2), 268–272. doi:10.1007/s12275-013-3126-5
- Huang, S., Kleerebezem, R., Rabaeu, K., and Ganigué, R. (2020). Open Microbiome Dominated by *Clostridium* and *Eubacterium* Converts Methanol into *i*-Butyrate and *n*-Butyrate. *Appl. Microbiol. Biotechnol.* 104 (11), 5119–5131. doi:10.1007/s00253-020-10551-w
- Imlay, J. A. (2006). Iron-sulphur Clusters and the Problem with Oxygen. *Mol. Microbiol.* 59 (4), 1073–1082. doi:10.1111/j.1365-2958.2006.05028.x
- Johnson, L. A., and Hug, L. A. (2019). Distribution of Reactive Oxygen Species Defense Mechanisms across Domain Bacteria. *Free Radic. Biol. Med.* 140, 93–102. doi:10.1016/j.freeradbiomed.2019.03.032
- Joshi, S., Robles, A., Aguiar, S., and Delgado, A. G. (2021). The Occurrence and Ecology of Microbial Chain Elongation of Carboxylates in Soils. *ISME J.* 15, 1907–1918. doi:10.1038/s41396-021-00893-2

- Kato, M. T., Field, J. A., and Lettinga, G. (1997). Anaerobe Tolerance to Oxygen and the Potentials of Anaerobic and Aerobic Cocultures for Wastewater Treatment. *Braz. J. Chem. Eng.* 14 (4), 395–407. doi:10.1590/s0104-66321997000400015
- Khademian, M., and Imlay, J. A. (2020). Do Reactive Oxygen Species or Does Oxygen Itself Confer Obligate Anaerobiosis? The Case of *Bacteroides thetaiotaomicron*. *Mol. Microbiol.* 114 (2), 333–347. doi:10.1111/mmi.14516
- Krab, K., Oltmann, L. F., and Stouthamer, A. H. (1982). Linkage of Formate Hydrogenylase with Anaerobic Respiration in *Proteus mirabilis*. *Biochim. Biophys. Acta (Bba) - Bioenerg.* 679 (1), 51–59. doi:10.1016/0005-2728(82)90254-7
- Krayzelova, L., Bartacek, J., Díaz, I., Jeison, D., Volcke, E. I. P., and Jenicek, P. (2015). Microaeration for Hydrogen Sulfide Removal during Anaerobic Treatment: a Review. *Rev. Environ. Sci. Biotechnol.* 14 (4), 703–725. doi:10.1007/s11157-015-9386-2
- Kucek, L. A., Nguyen, M., and Angenent, L. T. (2016). Conversion of L-Lactate into *n*-Caproate by a Continuously Fed Reactor Microbiome. *Water Res.* 93, 163–171. doi:10.1016/j.watres.2016.02.018
- Lambrecht, J., Cichocki, N., Schattenberg, F., Kleinstuber, S., Harms, H., Müller, S., et al. (2019). Key Sub-community Dynamics of Medium-Chain Carboxylate Production. *Microb. Cell Fact.* 18 (1), 92. doi:10.1186/s12934-019-1143-8
- Logroño, W., Popp, D., Kleinstuber, S., Sträuber, H., Harms, H., and Nikolausz, M. (2020). Microbial Resource Management for *Ex Situ* Biomethanation of Hydrogen at Alkaline pH. *Microorganisms* 8 (4), 614. doi:10.3390/microorganisms8040614
- Martin, W. F., and Sousa, F. L. (2015). Early Microbial Evolution: The Age of Anaerobes. *Cold Spring Harb. Perspect. Biol.* 8 (2), a018127. doi:10.1101/cshperspect.a018127
- Matassa, S., Verstraete, W., Pikaar, I., and Boon, N. (2016). Autotrophic Nitrogen Assimilation and Carbon Capture for Microbial Protein Production by a Novel Enrichment of Hydrogen-Oxidizing Bacteria. *Water Res.* 101, 137–146. doi:10.1016/j.watres.2016.05.077
- McCubbin, T., Gonzalez-Garcia, R. A., Palfreyman, R. W., Stowers, C., Nielsen, L. K., and Marcellin, E. (2020). A Pan-Genome Guided Metabolic Network Reconstruction of Five *Propionibacterium* Species Reveals Extensive Metabolic Diversity. *Genes* 11 (10), 1115. doi:10.3390/genes11101115
- Misra, H. P., and Fridovich, I. (1971). The Generation of Superoxide Radical during the Autoxidation of Ferredoxins. *J. Biol. Chem.* 246 (22), 6886–6890. doi:10.1016/s0021-9258(19)45929-2
- Mohr, T., Infantes, A., Biebinger, L., de Maayer, P., and Neumann, A. (2019). Acetogenic Fermentation from Oxygen Containing Waste Gas. *Front. Bioeng. Biotechnol.* 7, 433. doi:10.3389/fbioe.2019.00433
- Nguyen, D., and Khanal, S. K. (2018). A Little Breath of Fresh Air into an Anaerobic System: How Microaeration Facilitates Anaerobic Digestion Process. *Biotechnol. Adv.* 36 (7), 1971–1983. doi:10.1016/j.biotechadv.2018.08.007
- Oleskowicz-Popiel, P. (2018). Designing Reactor Microbiomes for Chemical Production from Organic Waste. *Trends Biotechnol.* 36 (8), 747–750. doi:10.1016/j.tibtech.2018.01.002
- Piwożarek, K., Lipińska, E., Hać-Szymańczuk, E., Kieliszek, M., and Ścibisz, I. (2018). *Propionibacterium* spp.—Source of Propionic Acid, Vitamin B12, and Other Metabolites Important for the Industry. *Appl. Microbiol. Biotechnol.* 102 (2), 515–538. doi:10.1007/s00253-017-8616-7
- Rao, J. U., Rash, B. A., Nobre, M. F., da Costa, M. S., Rainey, F. A., and Moe, W. M. (2012). *Actinomyces naturae* sp. nov., the First *Actinomyces* sp. Isolated from a Non-human or Animal Source. *Antonie Van Leeuwenhoek* 101 (1), 155–168. doi:10.1007/s10482-011-9644-4
- Sakamoto, M., Ikeyama, N., Toyoda, A., Murakami, T., Mori, H., Iino, T., et al. (2020). *Dialister hominis* sp. nov., Isolated from Human Faeces. *Int. J. Syst. Evol. Microbiol.* 70 (1), 589–595. doi:10.1099/ijsem.0.003797
- Scholz, C. F. P., and Kilian, M. (2016). The Natural History of Cutaneous *Propionibacteria*, and Reclassification of Selected Species within the Genus *Propionibacterium* to the Proposed Novel Genera *Acidipropionibacterium* gen. nov., *Cutibacterium* gen. nov. and *Pseudopropionibacterium* gen. nov. *Int. J. Syst. Evol. Microbiol.* 66 (11), 4422–4432. doi:10.1099/ijsem.0.001367
- Seeliger, S., Janssen, P. H., and Schink, B. (2002). Energetics and Kinetics of Lactate Fermentation to Acetate and Propionate via Methylmalonyl-CoA or Acrylyl-CoA. *FEMS Microbiol. Lett.* 211 (1), 65–70. doi:10.1111/j.1574-6968.2002.tb11204.x
- Smet, A., Cools, P., Krizova, L., Maixnerova, M., Sedo, O., Haesebrouck, F., et al. (2014). *Acinetobacter gandensis* sp. nov. Isolated from Horse and Cattle. *Int. J. Syst. Evol. Microbiol.* 64 (Pt 12), 4007–4015. doi:10.1099/ijss.0.068791-0
- Stamatopoulou, P., Malkowski, J., Conrado, L., Brown, K., and Scarborough, M. (2020). Fermentation of Organic Residues to Beneficial Chemicals: A Review of Medium-Chain Fatty Acid Production. *Processes* 8 (12), 1571. doi:10.3390/pr8121571
- Stiebritz, M. T., and Reiher, M. (2012). Hydrogenases and Oxygen. *Chem. Sci.* 3 (6), 1739. doi:10.1039/c2sc01112c
- Takahashi, N., Kalfas, S., and Yamada, T. (1994). The Role of the Succinate Pathway in Sorbitol Fermentation by Oral *Actinomyces viscosus* and *Actinomyces naeslundii*. *Oral Microbiol. Immunol.* 9 (4), 218–223. doi:10.1111/j.1399-302X.1994.tb00061.x
- Takahashi, N., and Yamada, T. (1999). Effects of pH on the Glucose and Lactate Metabolisms by the Washed Cells of *Actinomyces naeslundii* under Anaerobic and Aerobic Conditions. *Oral Microbiol. Immunol.* 14 (1), 60–65. doi:10.1034/j.1399-302X.1999.140108.x
- Takors, R., Kopf, M., Mampel, J., Bluemke, W., Blombach, B., Eikmanns, B., et al. (2018). Using Gas Mixtures of CO, CO<sub>2</sub> and H<sub>2</sub> as Microbial Substrates: the Do's and Don'ts of Successful Technology Transfer from Laboratory to Production Scale. *Microb. Biotechnol.* 11 (4), 606–625. doi:10.1111/1751-7915.13270
- Thauer, R. K., Kaster, A.-K., Goenrich, M., Schick, M., Hiromoto, T., and Shima, S. (2010). Hydrogenases from Methanogenic Archaea, Nickel, a Novel Cofactor, and H<sub>2</sub> Storage. *Annu. Rev. Biochem.* 79, 507–536. doi:10.1146/annurev.biochem.030508.152103
- Thompson, T. E., Conrad, R., and Zeikus, J. G. (1984). Regulation of Carbon and Electron Flow in *Propionispira arboris*: Physiological Function of Hydrogenase and its Role in Homopropionate Formation. *FEMS Microbiol. Lett.* 22 (3), 265–271. doi:10.1111/j.1574-6968.1984.tb00739.x
- Tomazetto, G., Hahnke, S., Wibberg, D., Pühler, A., Klocke, M., and Schlüter, A. (2018). *Proteiniphilum saccharofermentans* Str. M3/6T Isolated from a Laboratory Biogas Reactor Is Versatile in Polysaccharide and Oligopeptide Utilization as Deduced from Genome-Based Metabolic Reconstructions. *Biotechnol. Rep.* 18, e00254. doi:10.1016/j.btre.2018.e00254
- Vaishampayan, P., Miyashita, M., Ohnishi, A., Satomi, M., Rooney, A., La Duc, M. T., et al. (2009). Description of *Rummeliibacillus stabekisii* gen. nov., sp. nov. and reclassification of *Bacillus pycnus* Nakamura et al. 2002 as *Rummeliibacillus pycnus* comb. nov. *Int. J. Syst. Evol. Microbiol.* 59 (Pt 5), 1094–1099. doi:10.1099/ijss.0.006098-0
- Whitham, J. M., Tirado-Acevedo, O., Chinn, M. S., Pawlak, J. J., and Grunden, A. M. (2015). Metabolic Response of *Clostridium ljungdahlii* to Oxygen Exposure. *Appl. Environ. Microbiol.* 81 (24), 8379–8391. doi:10.1128/AEM.02491-15
- Yilmaz, P., Parfrey, L. W., Yarza, P., Gerken, J., Pruesse, E., Quast, C., et al. (2014). The SILVA and "All-Species Living Tree Project (LTP)" Taxonomic Frameworks. *Nucl. Acids Res.* 42 (Database issue), D643–D648. doi:10.1093/nar/gkt1209

**Conflict of Interest:** The authors declare that the research was conducted in the absence of any commercial or financial relationships that could be construed as a potential conflict of interest.

**Publisher's Note:** All claims expressed in this article are solely those of the authors and do not necessarily represent those of their affiliated organizations, or those of the publisher, the editors and the reviewers. Any product that may be evaluated in this article, or claim that may be made by its manufacturer, is not guaranteed or endorsed by the publisher.

Copyright © 2021 Baleeiro, Ardila, Kleinstuber and Sträuber. This is an open-access article distributed under the terms of the Creative Commons Attribution License (CC BY). The use, distribution or reproduction in other forums is permitted, provided the original author(s) and the copyright owner(s) are credited and that the original publication in this journal is cited, in accordance with accepted academic practice. No use, distribution or reproduction is permitted which does not comply with these terms.